Q1. The authors correctly point out that the laser beam cross-section in an optical tweezer system probes a radially averaged composition rather than a true volume-averaged concentration profile. This distinction is critical and handled skillfully in Section 3.3. Could the authors expand slightly on how sensitive this radial averaging assumption is to minor beam misalignment relative to the droplet core?

We thank the reviewer for raising the possibility that a slight beam misalignment relative to the droplet centre could affect the radial averaging assumption. We have further examined this issue from the perspectives of the optical trapping principle and model sensitivity.

First, under the working principle of single-beam gradient-force optical tweezers, stable trapping imposes a three-dimensional constraint on the droplet position. When a particle is displaced from the beam centre, the optical gradient force produces a restoring force directed toward the region of higher optical intensity, driving the trapped particle toward a stable equilibrium position near the beam centre (Neuman and Block, 2004). For aerosol droplets, a tightly focused beam can form a three-dimensional optical trap that confines aerosol particles in both the horizontal and vertical directions (Hopkins et al., 2004). Thus, under stable trapping conditions, the droplet is expected to remain confined near the centre of the laser beam.

Radial-averaging model for an off-centre laser beam

Although the droplet is confined as described above under ideal optical trapping conditions, weak gas-flow perturbations and other non-ideal experimental factors may still cause small, transient misalignment between the beam axis and the droplet centre. To evaluate the sensitivity of the radial-averaging treatment used in this study to such potential misalignment, we considered a deliberately large lateral displacement,

$$\beta = \frac{b}{R} = 0.2, \tag{S1}$$

where β denotes the dimensionless displacement, b is the lateral distance between the beam axis and the droplet centre, and R is the droplet radius. This configuration was introduced solely as a relatively conservative sensitivity test to determine the extent to which this geometrical effect could influence the retrieved D_w, even when the beam axis is displaced from the droplet centre by as much as 20% of the droplet radius.

When the laser-beam axis is laterally displaced from the droplet centre by a distance b, the beam traverses the spherical droplet along a chord that does not pass through the droplet centre. The half-length of this chord is

$$L = \sqrt{R^2 - b^2} = R\sqrt{1 - \beta^2}\,. \tag{S2}$$

Defining the z-axis along the direction of the laser beam, the radial distance from any point along the beam path to the droplet centre is

$$r = \sqrt{b^2 + z^2}\,. \tag{S3}$$

Accordingly, under an off-centre sampling geometry, the averaged D_2O fraction represented by the Raman signal can be expressed as

$$\Phi_\beta(t) = \frac{1}{C_s}\frac{1}{2L}\int_{-L}^{L} C(\sqrt{b^2 + z^2}, t)\, dz. \tag{S4}$$

where C_s is the concentration at the droplet surface. We retain the same spherical diffusion equation, constant surface concentration boundary condition, and quadratic initial radial concentration profile as in the main model, but reformulate the initial condition to account for the off-centre sampling geometry described above. Based on the initial path-averaged fraction, $\Phi_{\beta,0}$, along the off-centre beam path, the corresponding initial condition is

$$C(r,0) = C_s + \frac{3(1-\Phi_{\beta,0})C_s}{2(1-\beta^2)R^2} \cdot \left(\frac{r^2}{R^2} - 1\right). \quad \text{(S5)}$$

The modified model therefore retains the same underlying physical assumptions as the model presented in the main text; the only change is the laser beam's sampling path through the spherical concentration field. When β =0, the off-centre chord reduces to a diameter passing through the droplet centre, and the formulation correspondingly reduces to the original no-offset model used in the main text. Following the same procedure as in the main text, the spherically symmetric diffusion equation can be solved using the initial concentration profile together with the boundary condition, yielding the D_2O concentration distribution

$$\frac{C(r,t)}{C_s} = 1 + \frac{R}{r}\sum_{n=1}^{\infty} \frac{18(1-\Phi_{\beta,0})(-1)^n}{n^3\pi^3(1-\beta^2)} sin\left(\frac{n\pi r}{R}\right) exp\left(-\frac{n^2\pi^2 D_w t}{R^2}\right). \quad \text{(S6)}$$

Integrating this concentration field along the off-centre beam path defined above, and introducing the geometric function

$$I_n(\beta) = \frac{1}{\sqrt{1-\beta^2}} \int_0^{\sqrt{1-\beta^2}} \frac{sin[n\pi\sqrt{\beta^2+s^2}]}{\sqrt{\beta^2+s^2}} ds, \quad \text{(S7)}$$

gives the path-averaged D_2O fraction under the displaced-beam condition:

$$\Phi_\beta(t) = 1 + \sum_{n=1}^{\infty} \frac{18(1-\Phi_{\beta,0})(-1)^n}{n^3\pi^3(1-\beta^2)} I_n(\beta) exp\left(-\frac{n^2\pi^2 D_w t}{R^2}\right). \quad \text{(S8)}$$

As in the original model, the characteristic time is defined as

$$\tau = \frac{R^2}{\pi^2 D_w}. \quad \text{(S9)}$$

At $t = \tau$, the off-centre model retains a linear relationship between the D_2O fraction at the characteristic time and the initial fraction. The averaged D_2O fraction at the characteristic time is therefore

$$\Phi_\beta(\tau) = 1 + \sum_{n=1}^{\infty} \frac{18(1-\Phi_{\beta,0})(-1)^n}{n^3\pi^3(1-\beta^2)} I_n(\beta) exp(-n^2). \quad \text{(S10)}$$

For $\beta = 0.2$, numerical evaluation gives

$$\Phi_{0.2}(\tau) = 0.6142 + 0.3858\Phi_{0.2,0}. \quad \text{(S11)}$$

Impact on experimentally retrieved D_w

We subsequently applied the characteristic-time relationship rederived for $\beta = 0.2$ to the full experimental dataset and recalculated D_w for each experiment. The resulting values were then compared with those obtained using the original model ($\beta = 0$).

As shown in Fig. S1, across the full range of RH conditions investigated, the relative differences in D_w between the 20% offset model and the no-offset model were approximately 1.0–5.0%, with all experimental cases remaining below 5%. Moreover, we observed no systematic increase or decrease in deviation as RH changed. These results indicate that, even when a relatively large lateral offset is imposed as a sensitivity test, the resulting change in the retrieved D_w remains limited.

In summary, the single-beam optical trap itself constrains a stably trapped droplet to remain close to the beam centre. On this basis, we further imposed a lateral offset as large as 20% of the droplet radius to test the robustness of the radial-averaging assumption under a deliberately non-ideal sampling geometry. Even under this relatively large prescribed displacement, the differences between the recalculated D_w values and those obtained using the no-offset model remained below 5% for all experiments. We therefore conclude that the radial-averaging approximation adopted in this study is insensitive to the small beam-droplet misalignments that may occur in practice.

We added the corresponding sensitivity analysis and discussion to the Supplement of the revised manuscript.

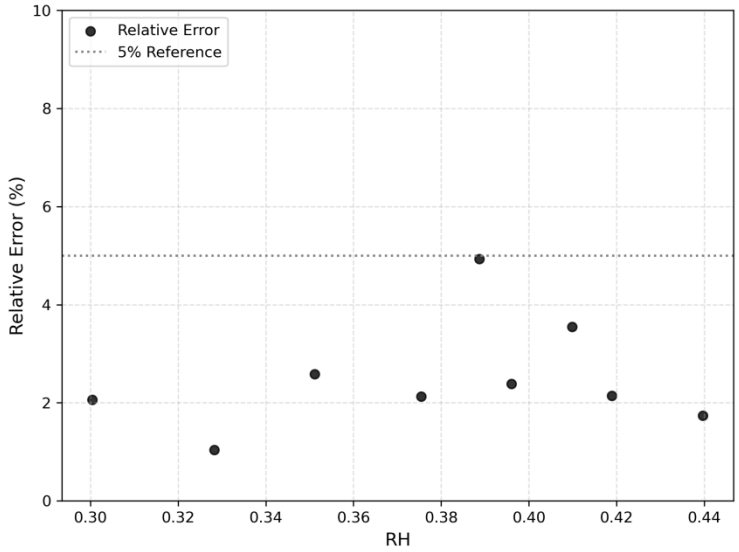

Figure S1: Relative difference in retrieved D_w between the lateral-offset and no-offset models.

Q2. Atmospheric relevance could be strengthened. The Introduction motivates the work by discussing aerosol viscosity. However, the manuscript would benefit from a more explicit discussion of how improved diffusion measurements translate into improved atmospheric models. For example, aerosol ageing, heterogeneous chemistry, SOA equilibration, etc. This broader context would increase the paper's impact.

We thank the reviewer for this valuable suggestion. We agree that a clearer connection between measurements of water diffusivity and their applications in atmospheric models helps better establish the broader significance of this study. Following the reviewer's suggestion, we added a new paragraph to the Introduction summarising the current use of the water diffusion coefficient in atmospheric aerosol models. The newly added text reads as follows:

The water diffusion coefficient is a key kinetic parameter governing water transport within aerosol particles. In kinetic models that account for intraparticle mass transfer, particles are typically partitioned radially into multiple concentric shells, and D_w is used to calculate the diffusive flux of water molecules between different radial positions. This allows the temporal evolution of particle water content and its radial distribution following changes in ambient relative humidity (RH) to be resolved, and further enables simulations of the associated changes in particle size and the time required to reach a new equilibrium state (Zobrist et al., 2011; Lienhard et al., 2014; Price et al., 2015). Such models have been applied to investigate the dynamic response of secondary organic aerosol to changes in ambient humidity (Lienhard et al., 2015; Price et al., 2015). In more comprehensive kinetic models of gas-particle interactions, such as the kinetic multi-layer model of gas-particle interactions in aerosols and clouds (KM-GAP), gas-phase transport of water molecules to the particle surface, interfacial exchange, and subsequent bulk diffusion within the particle are treated together with processes such as condensation, evaporation, and heat transfer, allowing the evolution of particle size and chemical reactions within the particle to be simulated (Shiraiwa et al., 2012). Intraparticle water diffusion can also be further coupled with cloud microphysical models. By incorporating water diffusivities that vary with temperature and water activity, such models can resolve the non-uniform distribution of water within highly viscous particles at low temperatures and its evolution during ascent of a cloud parcel, thereby enabling assessment of the effects of highly viscous aerosols on homogeneous ice nucleation (Fowler et al., 2020).

Q3. The compilation of data in Figure 5 is highly valuable. It would be useful to visually mark the glass transition RH for sucrose at 25°C directly onto the plot to emphasize exactly where the Stokes-Einstein breakdown becomes most prominent.

We thank the reviewer for this suggestion. We have reviewed the relevant literature and further clarified the relationship between the glass-transition relative humidity of the sucrose–water system and the departure from the Stokes–Einstein (SE) relation. The glass-transition relative humidity of sucrose aqueous aerosols has been reported to be approximately 24% RH at 298±2 K (Tong et al., 2011). A parameterisation of the glass transition for the sucrose–water system likewise gives a glass transition at a water activity of approximately 0.24 at 298.15 K (Zobrist et al., 2008). Accordingly, the revised Figure 5 now marks the glass-transition RH of sucrose at 25 °C (≈ 24 % RH) as a reference for understanding phase changes under low-RH conditions.

The water diffusivities measured in the present study correspond to roughly 30–45% RH, a range above the glass-transition RH of sucrose at 25 °C. Thus the system does not enter the glassy state under our experimental conditions. Nevertheless, the glass transition and the breakdown of the SE relation are not identical physical boundaries. Previous work has shown that water diffusion in the sucrose–water system can already deviate markedly from the classical SE relation before the glass transition is reached (Price et al., 2016). Previous experimental data for sucrose–water mixtures have been compared with diffusivities predicted from literature viscosity data using the SE relation (Chenyakin et al., 2017). The comparison shows that, even at a water activity of 0.60, the SE relation predicted diffusivities underestimate the measured values by 1–3 orders of magnitude, and that the discrepancy increases to 3–5 orders of magnitude when the water activity decreases to 0.38 (Chenyakin et al., 2017).

Therefore, the 30–45% RH range investigated in this study already falls within the high-viscosity regime in which substantial deviations of water diffusion from the classical SE prediction have been observed, with the discrepancy increasing as the system approaches the glass transition. In response to the reviewer's suggestion, the revised Figure 5 now indicates the glass-transition RH of sucrose at 25 °C, and the main text has been expanded to clarify the relationship of this reference point to both the 30–45% RH range of the present study and the observed breakdown of the SE relation.

References

Chenyakin, Y., Ullmann, D. A., Evoy, E., Renbaum-Wolff, L., Kamal, S., and Bertram, A. K.: Diffusion coefficients of organic molecules in sucrose–water solutions and comparison with Stokes–Einstein predictions, Atmos. Chem. Phys., 17, 2423–2435, https://doi.org/10.5194/acp-17-2423-2017, 2017.

Fowler, K., Connolly, P., and Topping, D.: Modelling the effect of condensed-phase diffusion on the homogeneous nucleation of ice in ultra-viscous particles, Atmos. Chem. Phys., 20, 683–698, https://doi.org/10.5194/acp-20-683-2020, 2020.

Hopkins, R. J., Mitchem, L., Ward, A. D., and Reid, J. P.: Control and characterisation of a single aerosol droplet in a single-beam gradient-force optical trap, Phys. Chem. Chem. Phys., 6, 4924, https://doi.org/10.1039/b414459g, 2004.

Lienhard, D. M., Huisman, A. J., Bones, D. L., Te, Y.-F., Luo, B. P., Krieger, U. K., and Reid, J. P.: Retrieving the translational diffusion coefficient of water from experiments on single levitated aerosol droplets, Phys. Chem. Chem. Phys., 16, 16677, https://doi.org/10.1039/C4CP01939C, 2014.

Lienhard, D. M., Huisman, A. J., Krieger, U. K., Rudich, Y., Marcolli, C., Luo, B. P., Bones, D. L., Reid, J. P., Lambe, A. T., Canagaratna, M. R., Davidovits, P., Onasch, T. B., Worsnop, D. R., Steimer, S. S., Koop, T., and Peter, T.: Viscous organic aerosol particles in the upper troposphere: diffusivity-controlled water uptake and ice nucleation?, Atmos. Chem. Phys., 15, 13599–13613, https://doi.org/10.5194/acp-15-13599-2015, 2015.

Neuman, K. C. and Block, S. M.: Optical trapping, Review of Scientific Instruments, 75, 2787–2809, https://doi.org/10.1063/1.1785844, 2004.

Price, H. C., Mattsson, J., Zhang, Y., Bertram, A. K., Davies, J. F., Grayson, J. W., Martin, S. T., O'Sullivan, D., Reid, J. P., Rickards, A. M. J., and Murray, B. J.: Water diffusion in atmospherically relevant α-pinene secondary organic material, Chem. Sci., 6, 4876–4883, https://doi.org/10.1039/C5SC00685F, 2015.

Price, H. C., Mattsson, J., and Murray, B. J.: Sucrose diffusion in aqueous solution, Phys. Chem. Chem. Phys., 18, 19207–19216, https://doi.org/10.1039/C6CP03238A, 2016.

Shiraiwa, M., Pfrang, C., Koop, T., and Pöschl, U.: Kinetic multi-layer model of gas-particle interactions in aerosols and clouds (KM-GAP): linking condensation, evaporation and chemical reactions of organics, oxidants and water, Atmos. Chem. Phys., 12, 2777–2794, https://doi.org/10.5194/acp-12-2777-2012, 2012.

Tong, H.-J., Reid, J. P., Bones, D. L., Luo, B. P., and Krieger, U. K.: Measurements of the timescales for the mass transfer of water in glassy aerosol at low relative humidity and ambient temperature, Atmos. Chem. Phys., 11, 4739–4754, https://doi.org/10.5194/acp-11-4739-2011, 2011.

Zobrist, B., Marcolli, C., Pedernera, D. A., and Koop, T.: Do atmospheric aerosols form glasses?, Atmos. Chem. Phys., 8, 5221–5244, https://doi.org/10.5194/acp-8-5221-2008, 2008.

Zobrist, B., Soonsin, V., Luo, B. P., Krieger, U. K., Marcolli, C., Peter, T., and Koop, T.: Ultra-slow water diffusion in aqueous sucrose glasses, Phys. Chem. Chem. Phys., 13, 3514, https://doi.org/10.1039/c0cp01273d, 2011.